Available online at www.sciencedirect.com
SCIENCE DIRECT®
Catalysis Today 93–95 (2004) 65–73
CATALYSIS TODAY
www.elsevier.com/locate/cattod

Methane dehydroaromatization over Mo/HZSM-5 catalysts in the absence of oxygen: effects of silanation in HZSM-5 zeolite

Hongmei Liu, Yong Li, Wenjie Shen, Xinhe Bao, Yide Xu*

State Key Laboratory of Catalysis, Dalian Institute of Chemical Physics, Chinese Academy of Sciences, 457 Zhongshan Road, P.O. Box 110, Dalian 116023, China

Abstract

TEOS as the exotic silicon source was used to modify HZSM-5 zeolite by chemical vapor deposition (CVD) in a vapor phase flow system. Mo/HZSM-5 catalysts prepared by using silicon-modified zeolite showed higher activity and stability than those prepared by using non-modified HZSM-5 zeolite in methane dehydro-aromatization (MDA) under non-oxidative conditions. The effect of silanation on the acid sites and the interaction between the Mo species and the acid sites have been studied by using FT-IR, NH_3-TPD and ^{1}H MAS NMR. The exotic silicon species not only selectively covered and eliminated almost all of the Brönsted acid sites on the external surface of HZSM-5 zeolite, but also affected the internal Brönsted acid sites, which are close to the channel openings. This results in an obvious decrease in the number of Brönsted acid sites per unit cell. In the MDA reaction, the Brönsted acid sites provided active sites not only for the polymerization and aromatization of the active intermedia, but also for the formation of carbonaceous deposits, which is a crucial factor leading to the deactivation of Mo/HZSM-5 catalyst. Only a small fraction of Brönsted acid sites, ca. 0.6 per unit cell, was required to accomplish the aromatization, and the superfluous free Brönsted acid sites would cause severe carbonaceous deposits under non-oxidative condition at a temperature as high as 973 K.

Keywords: Methane dehydroaromatization; Mo/HZSM-5; Silanation; Brönsted acid sites

1. Introduction

A good catalytic performance is achieved over Mo-modified HZSM-5 catalyst in the direct conversion of methane into aromatics such as benzene and toluene under non-oxidative conditions [1–5]. This reaction has received considerable attention since 1993. Many transition metals and different zeolites have been tested in an attempt to find a better catalyst [6–14]. However, up to now, the Mo/HZSM-5 catalyst is the best one among the tested catalysts at 973 K with the space velocity of methane around 1500 ml/g h [15].

It is generally accepted that the Mo oxide species are well dispersed on/in the HZSM-5 zeolite after calcination, and are reduced by methane in the initial period to form molybdenum carbide species, which are responsible for methane activation and the formation of C_2H_y species ($y < 4$) [1,16,17]. Moreover, the outstanding selectivity to benzene on Mo/HZSM-5 catalyst in this reaction is due to the unique channel structure of HZSM-5 with pore windows of 0.53 nm × 0.56 nm, close to the kinetic diameter of benzene. The zeolite channels play crucial roles in restraining the side reactions and controlling the product distribution [14].

The effect of the Brönsted acid sites of HZSM-5 zeolite on the catalytic performance of Mo/HZSM-5 catalyst has been well investigated. Ichikawa and coworkers reported that the catalytic performance of 3% Mo/HZSM-5 catalysts prepared using HZSM-5 zeolites with different SiO_2/Al_2O_3 ratios in MDA depended substantially on the Brönsted acidity of HZSM-5 zeolite, but had no any relationship with the Lewis acidity [18]. The Brönsted acid sites also play key role in the formation of carbonaceous deposits [19–23].

The location of Mo carbide species now has been specified. Iglesia and coworkers suggested that most of the MoC_x species should be resided in the channels [24–29]. This opinion has been further demonstrated with ^{1}H MAS NMR measurements on the Mo/HZSM-5 catalysts prepared by impregnation by Bao and coworkers [30]. Especially, as pointed out by Iglesia and coworkers that Mo species anchored on the external Brönsted acid sites were fully accessible to all molecules and had no protection against secondary re-

* Corresponding author. Tel.: +86 411 4379189; fax: +86 411 4694447.
E-mail address: xuyd@dicp.ac.cn (Y. Xu).

0920-5861/$ – see front matter © 2004 Elsevier B.V. All rights reserved.
doi:10.1016/j.cattod.2004.05.014

actions because of its catalytic behaviors of non-shape selective manners. Therefore, the appropriate pretreatment of HZSM-5 zeolite to selectively cover a part of the external surface is of importance to obtain a significant improvement in the selectivity to one-ring aromatics and an effective decrease in the formation of carbonaceous deposits on the Mo/HZSM-5 catalysts. Iglesia and coworkers reported that selective silanation of external acid sites with chemical liquid deposition on HZSM-5 by using large organosilane molecules could decrease the content of acid sites as well as the number of MoO_x species retained at the external surface, which was regarded as a key factor for coke formation during MDA. The formation rate of hydrocarbons on a 4% Mo/silica-modified HZSM-5 increased by about 30% in comparison with that on a 4Mo/HZSM-5 [31].

Silanation is one of the methods widely used to modify the OH groups on the external surface of zeolite. Many procedures of silanation on zeolite surface were suggested such as chemical vapor deposition (CVD) in a static vacuum system or in a vapor phase flow system and chemical liquid deposition (CLD). The deposition agents used as silicon source were usually bulky and silicon-containing compounds such as $SiCl_4$, tetramethoxysilane (TMOS) and tetraethoxysilane (TEOS), with corresponding kinetic molecular diameters of 0.71, 0.89 and 0.96 nm, respectively [32–35]. In the present work, the effect of silanation in HZSM-5 zeolite with TEOS by CVD on the catalytic performances of the Mo/HZSM-5 catalyst in the reaction of MDA was evaluated, and different techniques were applied to characterize the physical structure and chemical nature of the Mo-based silicon-modified HZSM-5 catalyst.

2. Experimental

2.1. Silanation method

The HZSM-5 zeolite with a SiO_2/Al_2O_3 ratio of 50 was supplied by Nankai University (Tianjin, China). The chemical vapor deposition (CVD) of tetraethoxysilane (TEOS) was carried out in a quartz tube. First, the original HZSM-5 was calcined at 773 K for 2 h to remove the water adsorbed on the zeolite. After the sample was cooled to 298 K, a stream of helium saturated with $Si(OC_2H_5)_4$ was switched to the tube. The silanation procedure was lasted for 8 h. The sample was subsequently calcined in air at 773 K for 8 h in order to decompose the organosilane precursors. To obtain appropriate level of SiO_2 deposition, the deposition–calcination cycles were repeated three times. The silicon-modified HZSM-5 zeolite is denoted as HZSM-5(Si), while the original zeolite is denoted as HZSM-5(O).

2.2. Catalyst preparation

The Mo/HZSM-5 catalysts with a Mo loading of 6 wt.% were prepared by impregnation method. In brief, HZSM-5 powders were impregnated with aqueous solutions containing a given amount of ammonia heptamolybdate (AHM), and then were dried at room temperature for 12 h. After further dried at 393 K for 2 h, the samples were calcined in air at 773 K for 6 h. The catalysts prepared by using HZSM-5(O) or HZSM-5(Si) as parent zeolites are denoted as 6Mo/HZSM-5(O) and 6Mo/HZSM-5(Si), respectively.

2.3. Catalytic evaluation

Catalyst evaluation was carried out in a fixed-bed reactor at 973 K and atmospheric pressure. Briefly, ca. 0.5 g of the catalyst was charged into a 10.0 mm i.d. quartz tubular reactor. Catalytic reactions were usually performed at 973 K at a space velocity of 1500 ml/g_{cat} h. On-line analysis of the effluent was performed with a Varian Star CP-3800 gas chromatograph using the Varian Star 5.5 data handling software. An amount of 10% N_2 was added to the methane feed as an internal standard. The methane conversion, selectivity of products and coke formation could be evaluated according to the carbon mass balance.

2.4. Catalyst characterization

Surface areas and micropore volumes of the samples were measured with the BET method on a Micromeritics ASAP-2000 instrument, based on adsorption isotherms at 77 K, and using 0.162 nm^2 for the cross-sectional area of the nitrogen molecules.

FT-IR spectra were recorded at room temperature on a Fourier transform infrared spectrometer (Nicolet Impact 410. The samples were diluted with KBr (ca. 1 wt.% of the samples used) and pressed into wafers.

X-ray diffraction (XRD) patterns were obtained in air on a Rigaku 200B diffractometer using Cu Kα radiation ($\lambda = 1.5418$ Å) at room temperature, with instrumental settings of 40 kV and 50 mA. The relative crystallinities of the samples were calculated based on the intensity of the peaks of angle $2\theta = 22–25^\circ$ in the XRD pattern [36].

X-ray Fluorescence spectroscopy (XRF) experiments were performed on a Philips MagiX X-ray Fluorescence spectrometer.

^{1}H MAS NMR experiments were carried out at 400.1 MHz on a Bruker DRX-400 spectrometer with BBI MAS probe and using 4 mm ZrO_2 rotors. Prior to the experiments, the samples were first dehydrated at 673 K for 20 h on a homemade apparatus for removing the water adsorbed, and then were put into the NMR rotors for measurement without exposing to air. Each sample was spun at 8 kHz and 200 scans were accumulated for each spectrum. The chemical shifts were referenced to a saturated aqueous solution of 4,4-dimethyl-4-silapentane sulfonate sodium (DSS). The number of Brönsted acid sites per unit cell in the parent zeolite was calculated from the corresponding unit cell composition. The number of Brönsted acid sites per unit cell of the Mo/HZSM-5 catalysts after calcinations

was estimated by comparing the peak areas of the ^{1}H MAS NMR spectra with the corresponding parent zeolite.

The temperature-programmed desorption of ammonia (NH_3-TPD) was performed to determine the acidity of different samples. The sample (0.2 g) was first flushed with He at 873 K for 30 min, then cooled to 423 K and saturated with NH_3. After NH_3 exposure, the sample was He-purged until equilibrium, and then heated from 423 to 923 K at a heating rate of 10 K/min. A Quantachrome CHEMBET-3000 instrument was employed to monitor the amount of ammonia in the effluent.

2.5. Characterization of carbonaceous deposits: TGA and TPO

TGA profiles were recorded on a Perkin-Elmer TG 1700 instrument. The used catalyst of ca. 0.02 g was heated in an air stream (30 ml/min) from 313 to 1023 K at a heating rate of 10 K/min.

The temperature-programmed oxidation (TPO) study was carried out in a U-shaped quartz tubular micro-flow reactor. The used catalyst of 0.1 g was heated in a He stream to remove the adsorbed water and flushed with the mixture stream of 10% O_2/He (30 ml/min) at room temperature for 1 h. Then, TPO was conducted from room temperature to 1073 K in a mixture stream at a heating rate of 20 K/min. The products were detected and analyzed by a Balzers QMS-200 on-line multi-channel quadruple mass spectrometer. During the temperature ramp, the evolved species were monitored at $m/e = 28$(CO), 32(O_2) and 44(CO_2), respectively. The data from TGA and TPO were calculated and analyzed in the same methods as described in our previous paper [21,37]. Briefly, data at $m/e = 28$ originally recorded was corrected by subtracting the contribution from the CO_2 signal to get the data of CO. Then the data of CO multiplied by its respective response parameter was added to that of CO_2 to get the data of total carbon oxides.

3. Results and discussion

3.1. IR, BET, XRF and XRD results

The effects of silanation on the framework structure of HZSM-5 zeolite and the corresponding Mo/HZSM-5 catalyst were characterized by infrared spectroscopy and the IR absorbance spectra are illustrated in Fig. 1. The absorption bands at 1226, 1100, 795, 547, 453 cm^{-1} are considered as the characteristic signals for framework vibration of HZSM-5 zeolite. Especially, the band at 1226 cm^{-1} is sensitive to the ratio of framework Si/Al and the decrease of framework Al species can lead to a shift of this signal to a higher frequency, as reported in [38]. According to the IR spectra recorded from the HZSM-5(O) zeolite and the 6Mo/HZSM-5(O) catalyst, the fundamental framework structure and bulk Si/Al ratio of the zeolite are hardly affected by the loading of Mo species. On the other hand, all the structure-sensitive bands in the spectrum of the HZSM-5(Si) and 6Mo/HZSM-5(Si) samples are similar to those of HZSM-5(O), suggesting that the exotic silicon species did not severely destroy the basic structure of HZSM-5.

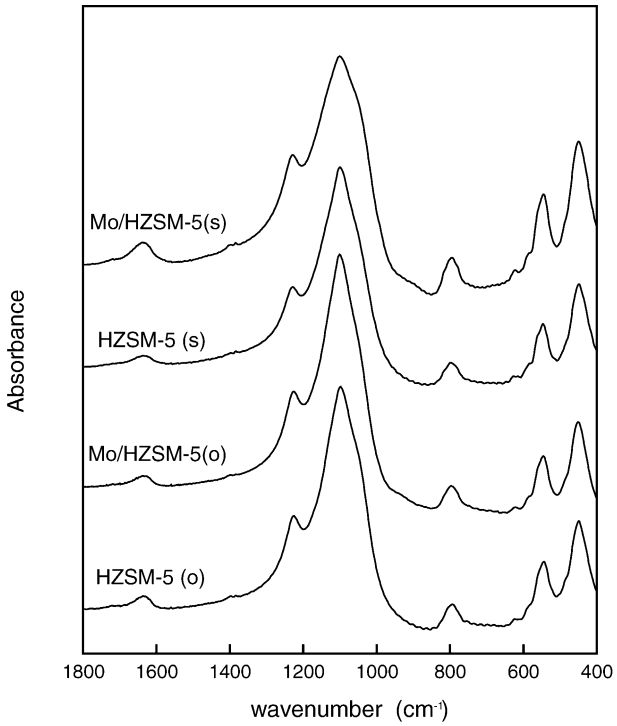

Fig. 1. FT-IR spectra of silicon-modified and unmodified HZSM-5 zeolites, as well as their 6 wt.% Mo/HZSM-5 catalysts.

The surface areas and micropore volumes of the samples are listed in Table 1. The silanation in HZSM-5 zeolite led to a decrease in both the BET surface areas and micropore volumes. O'Connor and coworkers investigated the acidity of HZSM-5 zeolite modified with silanation by CVD or CLD of TEOS [32]. The authors claimed that the total acidity of the sample treated by CVD decreased significantly based on their pyridine-TPD measurements. Meanwhile, the diffusional properties of the silicon-modified HZSM-5 were quite different from those of non-modified zeolite. They considered this phenomenon as a result of the replacement of partial acid sites located near the openings by the exotic silicon species to narrow or block the pores. A decrease in BET surface area and in micropore volume of HZSM-5 zeolite shows that the blockage of zeolite channels occurred in the process of silicon modification. It is not surprising that the introduction of Mo species on HZSM-5 zeolite could also result in a slight blockage of zeolite channels, owing to the migration of Mo species into the channels of zeolite.

The XRD patterns of HZSM-5(Si) was similar to that of HZSM-5(O). There were only peaks characteristic for HZSM-5 and no any new characteristic signals appeared in

Table 1
Numerical results of BET, XRF and XRD measurements

Sample	Surface area[a] (m^2/g)	Micropore volume[a] (cc/g)	Mo containing[b] (wt.%)	Mo/Si in bulk[b]	Si/Al in bulk[b]	Relative crystallinity[c] (%)
HZSM-5 (o)	342	0.17	–	–	23.4	100
Mo/HZSM-5 (o)	281	0.15	5.68	0.04	23.1	82
HZSM-5 (s)	312	0.16	–	–	23.3	88
Mo/HZSM-5 (s)	255	0.14	5.46	0.04	23.2	81

[a] Based on the date of BET measurement.
[b] Based on the XRF results.
[c] Based on the XRD data.

the pattern of the HZSM-5(Si) zeolite, revealing that the exotic silicon species were well dispersed on the surface of HZSM-5. At the same time, the signals corresponding to Mo species could not be observed in the patterns of these two 6Mo/HZSM-5 catalysts, indicating that the molybdenum species were highly dispersed. Moreover, the relative crystallinity of the HZSM-5(Si) zeolite decreased to 88% of that of the HZSM-5(O) sample. Obviously, the introduction of the exotic silicon species on HZSM-5 could cause a partial destruction of the zeolite framework structure.

3.2. NH_3-TPD and ^1H MAS NMR results

The NH_3-TPD profiles of HZSM-5 zeolites and 6Mo/HZSM-5 catalysts are shown in Fig. 2. By deconvoluting, the original spectrum of HZSM-5(O) sample exhibited three different peaks at about 556, 659 and 759 K, respectively (in Fig. 2(a)). It is generally accepted that, the peak at low temperature (556 K) is associated with the physisorbed ammonia [39], while the one at 759 K has been attributed to the ammonia adsorbed on the strong acid sites [40–42]. The adscription of the peak at moderate temperature in the NH_3-TPD profiles is still uncertain. It is assigned to the desorbed ammonia on extra-framework Al [43] or Si–OH [44]. It is also possible to attribute it to the ammonia adsorbed on the medium acid sites, which are created by the interaction between Mo species and the Brönsted acid sites. The peak areas, which corresponding to the amounts of various acid sites, can be estimated and the results are listed in Table 2. As expected the loading of 6 wt.% Mo species led to a decrease in the total amount of desorbed ammonia. Both the areas of the high and low temperature peaks in the NH_3-TPD profile of 6Mo/HZSM-5 decreases to ca. 70% of those of the HZSM-5 samples, indicating that a number of strong (mainly Brönsted acid sites) and weak acid sites on the catalyst are covered by the Mo species. On the other hand, the peak area at the moderate temperature increased evidently after the loading of Mo species, and the peak temperature shifted from 659 to 629 K. Probably, the increase was related with the interaction between Mo species and the acid sites of HZSM-5 zeolite.

The effect of silanation on the acidity of HZSM-5 zeolite was rather evident. All three peaks in the NH_3-TPD profile of HZSM-5(Si) are smaller than the corresponding peaks in the profile of HZSM-5(O) as demonstrated in Fig. 2(c). The

Table 2
Peak temperatures and areas of NH_3-TPD profiles

Sample	Peak temperature (K)			Peak area (a.u.)		
	T_1	T_2	T_3	A_1	A_2	A_3
HZSM-5 (o)	556	659	759	518	159	510
Mo/HZSM-5 (o)	550	629	757	361	372	371
HZSM-5 (s)	544	624	735	256	125	248
Mo/HZSM-5 (s)	550	626	745	259	139	173

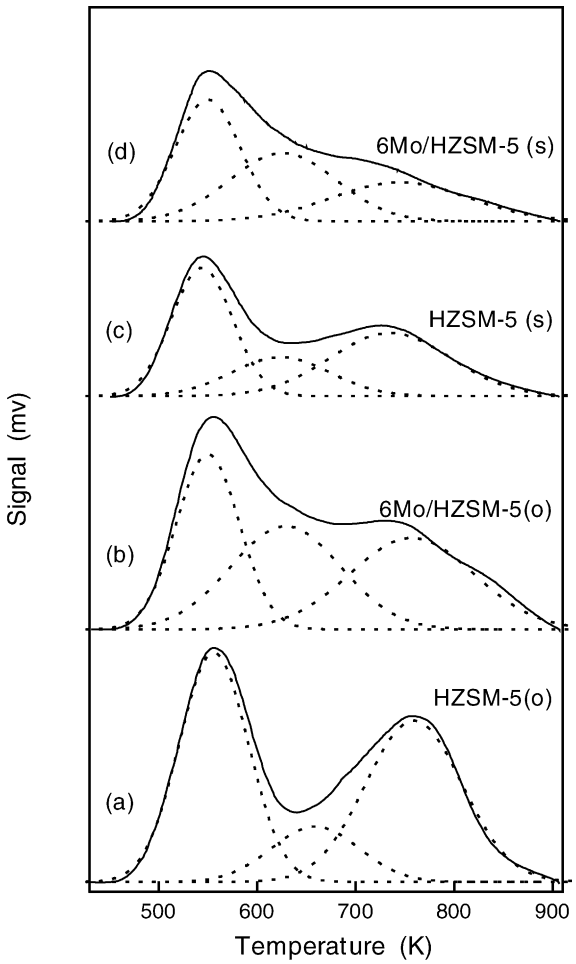

Fig. 2. NH_3-TPD profiles of silicon-modified and unmodified HZSM-5 zeolites, as well as their 6 wt.% Mo/HZSM-5 catalysts.

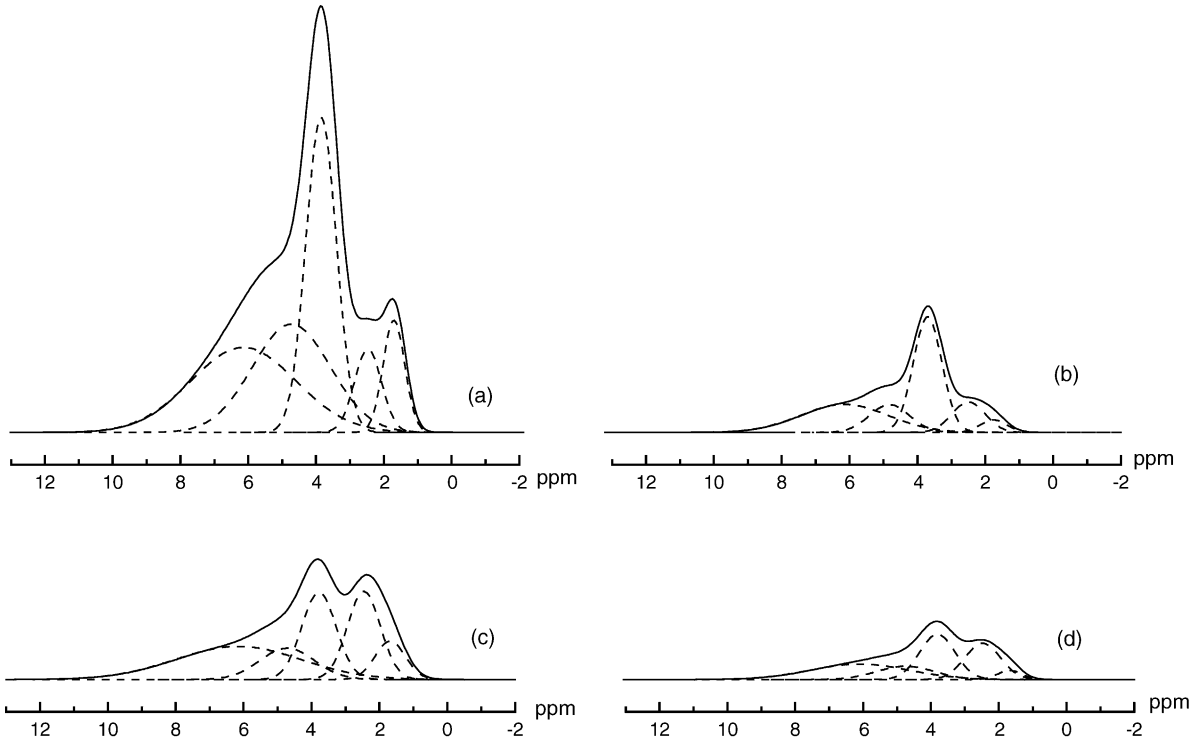

Fig. 3. ^{1}H spin-echo MAS NMR spectra of silicon-modified and unmodified HZSM-5 zeolites, as well as their 6 wt.% Mo/HZSM-5 catalysts: (a) for HZSM-5 (o); (b) for Mo/HZSM-5 (o); (c) for HZSM-5 (s); (d) for Mo/HZSM-5 (s).

amount of physisorbed ammonia on HZSM-5(Si) decreased to 49% of that on HZSM-5(O) sample, and the ammonia adsorbed on strong acidic hydroxyl groups decreased to 48%. At the same time, the area at moderate temperature had a slight reduction from 159 to 125. The results give evidence that more than half of the strong acid sites of the HZSM-5(O) zeolite were covered by the exotic silicon species. In addition, the introduction of Mo species on the HZSM-5(Si) resulted in a further decrease in the strong acid sites from 48% to 34%.

In order to obtain more information about the effect of the exotic silicon species on the acid sites of the HZSM-5 zeolite and Mo/HZSM-5 catalyst, ^{1}H MAS NMR was performed. The ^{1}H MAS NMR spectra of HZSM-5 zeolites before and after silicon modification as well as their Mo-containing catalysts are shown in Fig. 3.

As previously reported [45–50], the typical ^{1}H MAS NMR spectrum of dehydrated HZSM-5 zeolite without any modification after deconvolution usually exhibited five characteristic resonance peaks. The high-field signal with a chemical shift of 1.7 ppm is due to external Si–OH groups, the peak at $\delta = 2.4$ ppm is attributed to the extra-framework Al–OH as described in [47,48]. The other two low-field peaks at δ =3.8 and 6.0 ppm are attributed to Brönsted acid sites, the former is associated with the bridging OH groups in the form of ≡Al–OH–Si≡, and the latter is attributed to the Brönsted acid sites affected by additional electrostatic interaction of the oxygen atoms in the zeolite framework [45–50]. In addition, the peak with a chemical shift of 4.7 ppm is associated with trace water molecules located in the zeolite cages [51]. The variation in the number of different kinds of hydroxyl groups per unit cell on the HZSM-5 zeolite before and after silanation and the corresponding 6Mo/HZSM-5 catalysts are listed in Table 3. By comparing the Fig. 3(b) with (a), it is obvious that the introduction of Mo species caused a significant decrease in the total ^{1}H signals intensity. The change in the number of Brönsted acid sites was the most evident, decreasing from 3.70 to 1.12 per u.c. At the same time, the intensities of the signals at $\delta = 1.7$ and 2.4 ppm also displayed a significant reduction. These results give evidence that the introduction of Mo species will affect all kinds of hydroxyl groups on the surface of HZSM-5 zeolite. Moreover, the signals at δ = 3.8 and 6.0 ppm in the ^{1}H MAS NMR spectrum of the HZSM-5(Si) zeolite were much weaker than those in the spectrum of the HZSM-5(O) one.

Both of the NH_3-TPD and ^{1}H MAS NMR results indicate that more than half of the proton acidity was passivated during the procedure of silanation, revealing that the exotic silicon species not only can cover on the Brönsted acid sites located on the external surface of the HZSM-5 zeolite and passivate these acid site, but also can replace a number of acid sites located at the openings of channels to result in a significant decrease of proton acid sites, as suggested in [32].

The effect of silanation on the terminal Si–OH groups of HZSM-5 zeolite was also obvious, and the amount of this kind of hydroxyls decreased from 0.49 to 0.23 per unit

Table 3
Numerical results of ^{1}H MAS NMR experiments on HZSM-5 zeolite and Mo/HZSM-5 catalysts

Sample	Number of hydroxyls per unit cell					Number of B acid site per u.c.[a]
	*B*2 (6.0)	Water (4.7)	*B*1 (3.8)	Al–OH (2.3)	Si–OH (1.7)	
HZSM-5 (o)	1.78	1.68	1.92	0.45	0.49	3.70
Mo/HZSM-5 (o)	0.49	0.21	0.63	0.20	0.07	1.12
HZSM-5 (s)	0.84	0.35	0.59	0.58	0.23	1.43
Mo/HZSM-5 (s)	0.30	0.14	0.31	0.24	0.05	0.61

[a] The number of Brönsted acid sites per unit cell = *B*1 + *B*2.

cell. Evidently, the exotic silicon species not only deposited on Brönsted acid sites, but also covered a part of Si–OH groups of HZSM-5. On the other hand, the signal with a chemical shift of 2.4 ppm increased significantly in the ^{1}H MAS NMR spectrum of HZSM-5(Si) zeolite, compared with HZSM-5(O) sample. The result of ^{1}H MAS NMR indicates that, a portion of framework Al species on HZSM-5 zeolite was extracted to form extra-framework Al during the processes of chemical vapor deposition and the succeeding calcination. The loading of Mo species on HZSM-5(Si) caused a further reduction in the number of proton acid sites, from 1.43 to 0.61 per unit cell. Obviously, the Brönsted acid sites eliminated by Mo species (0.82 per unit cell) were in the channels of HZSM-5(Si) zeolite, since the Brönsted acid sites located on the external surface had been covered by the exotic silicon species before the introduction of the Mo species. However, the decrement of Brönsted acid sites was much larger when the Mo species was introduced on HZSM-5(O) zeolite. It is suggested that there is much more Mo species associated with Brönsted acid sites on Mo/HZSM-5(O) than on Mo/HZSM-5(Si). However, in the latter case the Mo species are mainly located in the channels of HZSM-5 zeolite, while in the former case the Mo species are resided on the external surface and in the channels.

3.3. Effect of silanation on the catalytic behavior of the Mo/HZSM-5 catalyst in MDA

The catalytic performance of the MDA on the 6Mo/HZSM-5(Si) catalyst at 973 K and 1500 ml/g_{cat} h was much better than that on the 6Mo/HZSM-5(O) catalyst, and the results are shown in Fig. 4. As illustrated, the rate of methane conversion over 6Mo/HZSM-5(O) decreased from 2.7 to 0.8 μmol/g_{cat} s after running the reaction for 24 h. However, on the 6Mo/HZSM-5(Si) catalyst, the depletion rate of methane maintained at 1.4 μmol/g_{cat} s after 24 h on stream. The semi-logarithmic plot of the rate of methane conversion on these two catalysts are shown in Fig. 5(A). The first-order deactivation rate constant, based on the data of methane depletion, was prominently smaller on the 6Mo/HZSM-5(Si) catalyst ($0.43 \times 10^{-5}\,s^{-1}$) than on the 6Mo/HZSM-5(O) catalyst ($1.1 \times 10^{-5}\,s^{-1}$). In the same way, the formation of one-ring hydrocarbon (including benzene, toluene and xylene) over the 6Mo/HZSM-5(Si) was much more stable than on the on the 6Mo/HZSM-5(O) catalyst. On the 6Mo/HZSM-5(Si) catalyst, the BTX (dominatingly benzene) formation rate decreased from the highest point (1.6 μmol/g_{cat} s) to 1.2 μmol/g_{cat} s after 24 h on stream with a deactivation rate constant of $0.35 \times 10^{-5}\,s^{-1}$.

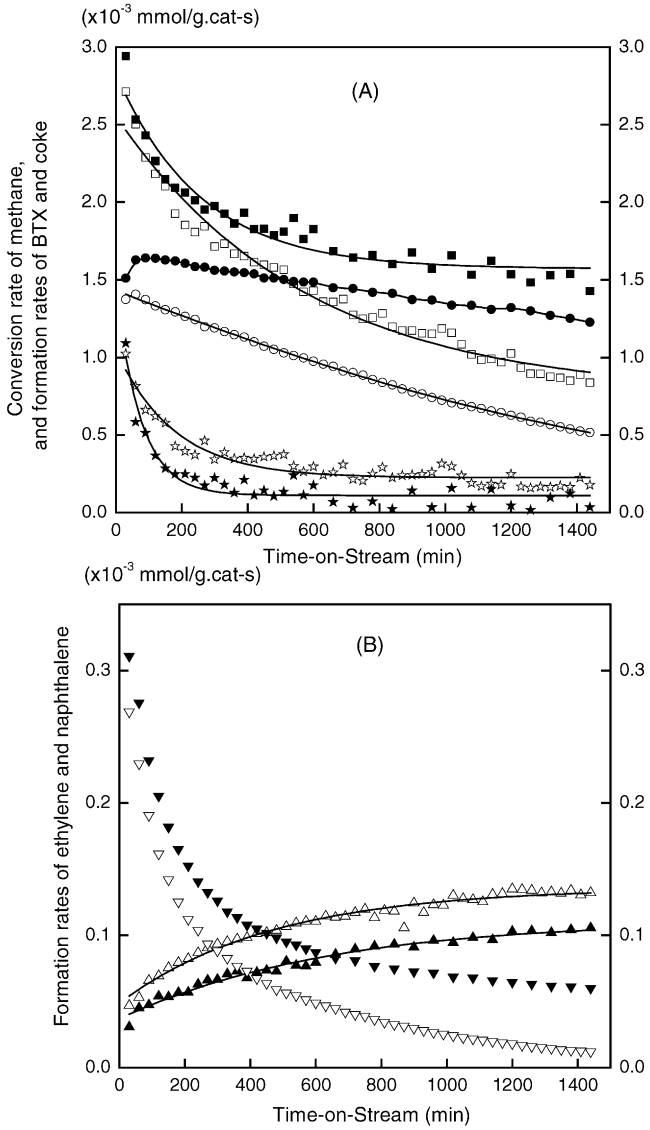

Fig. 4. Catalytic performances of the Mo/HZSM-5 (o) and Mo/HZSM-5(Si) catalysts: (■) for methane conversion; (●) for BTX formation; (★) for coke formation; (▼) for naphthalene formation; (▲) for ethylene formation.

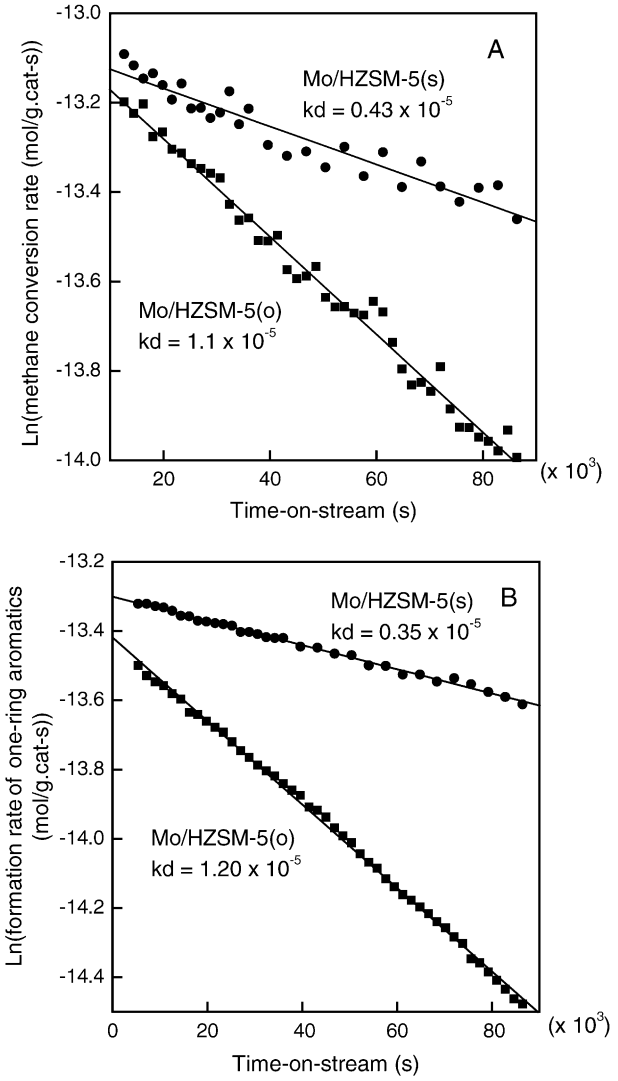

Fig. 5. Rates of methane conversion and BTX formation over Mo/HZSM-5 catalysts prepared using the silicon-modified zeolite and unmodified HZSM-5 zeolites. (the values of k_d are calculated from the slope of semilogarithmic plot).

However, the deactivation rate constant increased to $1.2 \times 10^{-5}\,s^{-1}$ on the 6Mo/HZSM-5(O) as shown in Fig. 5(B).

As indicated in ^{1}H MAS NMR experiments, the number of Brönsted acid sites per unit cell is about 1.12 was retained on the 6Mo/HZSM-5(O) catalyst, and the number of Brönsted acid sites per unit cell was 0.61 on the 6Mo/HZSM-5(Si) catalyst. However, the latter catalyst exhibited a higher stability in the reaction of MDA than the former one, and the formation of carbonaceous deposits was suppressed over the 6Mo/HZSM-5(Si) catalyst, which, as indicated, with less Brönsted acid sites. This implies that the number of Brönsted acid sites per unit cell needed in the oligmerization, cyclization and aromatization of the active intermediates is quite small. If there were too many Brönsted acid sites in the channels, the formation rate of carbonaceous deposits will be accelerated as reported in our previous work [37]. Therefore the catalyst will be deactivated very quickly. The exotic silicon species not only eliminated the external Brönsted acid sites to suppress the non-shape selective reactions, but also covered some excess Brönsted acid sites located on the mouths of the zeolite channels. Profiting from the silicon modification, the 6Mo/HZSM-5(Si) catalyst exhibited a higher selectivity to one-ring aromatics and a better stability in the reaction of MDA than the Mo/HZSM-5(O)catalyst.

Furthermore, the results of catalytic evaluation indicated that more naphthalene, but less ethylene, formed over the 6Mo/HZSM-5(Si) than on the 6Mo/HZSM-5(O) catalyst. This results imply that the formation of naphthalene and benzene need the same active sites and, perhaps, through the same reaction pathway.

3.4. Characterization of the coke formed during the reaction

Fig. 6(A) and (B) shows the TPO profiles (after correction) of the used 6Mo/HZSM-5 catalysts after running the reaction for 10 and 24 h, respectively. The profiles of total carbon oxides were deconvoluted, and the peak temperatures as well as the corresponding amounts of the carbonaceous deposits species burnt-off at different temperature are listed in Table 4. It is evident that the profiles of both the coked 6Mo/HZSM-5(O) and 6Mo/HZSM-5(Si) catalyst after running the reaction for 10 h show two peaks at the peak temperatures of 741 and 816 K (see Fig. 6(A)). The amount of the coke formed on the 6Mo/HZSM-5(Si) was much less than on the 6Mo/HZSM-5(O) catalyst, especially the coke burnt at high temperature. The amount of this kind of coke was 19.3 mg/g_{cat}. On the 6Mo/HZSM-5(O) catalyst, but only 6.1 mg/g_{cat}. On the Mo/HZSM-5(Si) catalyst. With the increase in time on stream, the carbon species deposited increased, either on the 6Mo/HZSM-5(O) catalyst or on the 6Mo/HZSM-5(Si). However, the increase of the coke on the 6Mo/HZSM-5(Si) was not as so obviously as on the 6Mo/HZSM-5(O). After 24 h on stream the amount of the coke formed on the 6Mo/HZSM-5(O) catalyst was about as three times as that on the 6Mo/HZSM-5(Si) catalyst. The formation of coke burnt at a high temperature was obviously prevented on the 6Mo/HZSM-5(Si) catalyst as shown in Fig. 6.

The carbonaceous deposits burnt at high temperature were mainly formed on the Brönsted acid sites and were responsible for the gradual deactivation of the catalyst. While the coke burnt at a low temperature was primarily deposited on the Mo species. The deactivation of Mo/HZSM-5 catalyst is basically independent of the latter kind of carbon species [21,23]. The amount of Brönsted acid sites remained on the surface of 6Mo/HZSM-5(Si) is much less than that on 6Mo/HZSM-5(O), as demonstrated by NH_3-TPD and ^{1}H MAS NMR experiments. Therefore, the formation of coke deposited on proton acid sites was dramatically suppressed. At the same time, both the conversion of methane and formation of one-ring aromatics were improved and stabilized

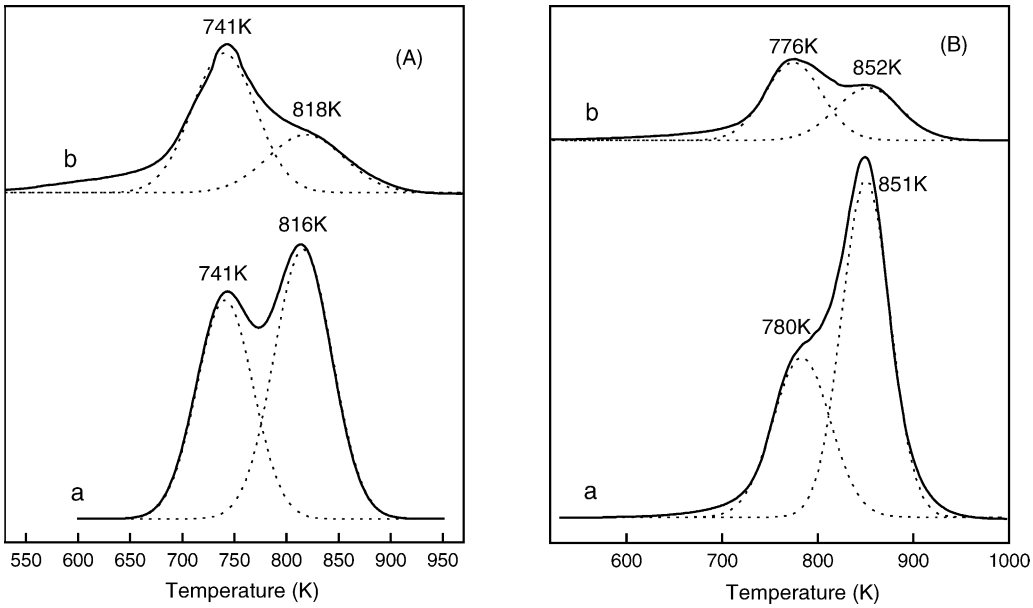

Fig. 6. TPO profiles and the deconvolution results of the used Mo/HZSM-5 catalysts: (a) for Mo/HZSM-5 (o) catalyst; (b) for Mo/HZSM-5 (s) catalyst, after the reaction run for (A) 10 h; (B) 24 h.

Table 4
Peak temperatures of the TPO profiles and the amount of coke formed on the used Mo/HZSM-5 (o) and Mo/HZSM-5(Si) catalysts after a 10 h reaction or a 24 h reaction

Sample	Peak temperature, K		The amount of coke, mg/g_{cat}		
	Low temperature	High temperature	Low temperature	High temperature	Total[a]
Mo/HZSM-5 (o) (10 h)	741	816	15.4	19.3	34.7
Mo/HZSM-5 (s) (10 h)	741	818	12.2	6.1	18.3
Mo/HZSM-5 (o) (24 h)	780	851	27.4	49.7	77.1
Mo/HZSM-5 (s) (24 h)	776	852	15.2	11.7	26.9

[a] Measured by TGA experiments.

on the 6Mo/HZSM-5(Si) catalyst. All the results give evidence that too many Brönsted acid sites left are undesirable for the MDA reaction.

4. Conclusions

The exotic silicon species not only could cover the Brönsted acid sites on the external surface of HZSM-5 zeolite, but also could replace a part of the Brönsted acid sites located near the openings. The silanation of HZSM-5 zeolite significantly improves the activity and stability of Mo/HZSM-5 catalyst for methane conversion and aromatics formation, as well as suppresses the deposition of carbonaceous species on the surface of the catalyst. The Brönsted acid sites not only provide active sites for the polymerization and aromatization of the active intermediates, but also play an important role in the formation of carbonaceous deposits. The number of Brönsted acid sites needed in the reaction of MDA is less than 0.6 per unit cell, and a larger number of Brönsted acid sites on the external surface and in the channels of HZSM-5 are undesirable.

Acknowledgements

Financial supports from the Ministry of Science and Technology of China under the contract G1999022406 and from the BP-China Joint Center are gratefully acknowledged.

References

[1] L. Wang, L. Tao, M. Xie, G. Xu, J. Huang, Y. Xu, Catal. Lett. 21 (1993) 35.
[2] Y. Xu, L. Lin, Appl. Catal. A 188 (1999) 53.
[3] J.H. Lunsford, Catal. Today 63 (2000) 165.
[4] Y. Shu, M. Ichikawa, Catal. Today 71 (2001) 55.
[5] Y. Xu, X. Bao, L. Lin, J. Catal. 216 (2003) 386.
[6] Y. Xu, S. Liu, L. Wang, M. Xie, X. Guo, Catal. Lett. 30 (1995) 135.
[7] Y.Y. Shu, D. Ma, L.Y. Xu, Y.D. Xu, X.H. Bao, Catal. Lett. 70 (2000) 67.
[8] Y.Y. Shu, D. Ma, X.C. Liu, X.W. Han, Y.D. Xu, X.H. Bao, J. Phys. Chem. B 104 (2000) 8245.
[9] S. Liu, Q. Dong, R. Ohnishi, M. Ichikawa, Chem. Commun. (1997) 1455.
[10] L.S. Wang, R. Ohnishi, M. Ichikawa, J. Catal. 190 (2000) 276.
[11] J. Zeng, Z. Xiong, H. Zhang, G. Lin, K. Tsai, Catal. Lett. 53 (1998) 119.

[12] B.M. Weckhuysen, D. Wang, M.P. Rosynek, J.H. Lunsford, J. Catal. 175 (1998) 338.
[13] B.M. Weckhuysen, D. Wang, M.P. Rosynek, J.H. Lunsford, J. Catal. 175 (1998) 347.
[14] C.L. Zhang, S. Li, Y. Yuan, W.S. Zhang, T.H. Wu, L.W. Lin, Catal. Lett. 56 (1998) 207.
[15] Y. Shu, Y. Xu, S. Wong, L. Wang, X. Guo, J. Catal. 170 (1997) 11.
[16] F. Solymosi, J. Cserenyi, A. Szoke, T. Bansagi, A. Dszko, J. Catal. 165 (1997) 150.
[17] D. Wang, J.H. Lunsford, M.P. Rosynek, J. Catal. 169 (1997) 347.
[18] S. Liu, L. Wang, R. Onishi, M. Ichikawa, J. Catal. 181 (1999) 175.
[19] B. Weckhuysen, M. Rosynek, J. Lunsford, Catal. Lett. 52 (1998) 31.
[20] H. Jiang, L. Wang, W. Cui, Y. Xu, Catal. Lett. 57 (1999) 95.
[21] H. Liu, T. Li, B. Tian, Y. Xu, Appl. Catal. A 213 (2001) 103.
[22] B. Liu, Y. Yang, A. Sayari, Appl. Catal. A 214 (2001) 95.
[23] Y. Lu, Z. Xu, Z. Tian, T. Zhang, L. Lin, Catal. Lett. 62 (1999) 215.
[24] D.G. Barton, S.L. Soled, G.D. Meitzner, G.A. Fuentes, E. Iglesia, J. Catal. 181 (1999) 57.
[25] G. Meitzner, E. Iglesia, Catal. Today 53 (1999) 433.
[26] R.W. Borry, Y.H. Kim, A. Huffsmith, J.A. Reimer, E. Iglesia, J. Phys. Chem. B 103 (1999) 5787.
[27] Y.H. Kim, R.W. Borry, E. Iglesia, J. Ind. Eng. Chem. 6 (2000) 72.
[28] Y.H. Kim, R.W. Borry, E. Iglesia, Micropor. Mesopor. Mater. 35/36 (2000) 495.
[29] W. Li, G.D. Meitzner, R.W. Borry, E. Iglesia, J. Catal. 191 (2000) 373.
[30] D. Ma, Y. Shu, W. Zhang, X. Han, Y. Xu, X. Bao, Angew. Chem. 39 (2000) 2928.
[31] W. Ding, G.D. Meitzner, E. Iglesia, J. Catal. 206 (2002) 14.
[32] R.W. Weber, K.P. Möller, M. Unger, C.T. O'Connor, Micropor. Mesopor. Mater. 23 (1998) 179.
[33] R.A. Shaikh, S.G. Hegde, M. Unger, A.A. Behlekar, B.S. Rao, Catal. Today 49 (1999) 201.
[34] R.W. Weber, K.P. Möller, C.T. O'Connor, Micropor. Mesopor. Mater. 35/36 (2000) 533.
[35] H. Manstein, K.P. Möller, W. Böhringer, C.T. O'Connor, Micropor. Mesopor. Mater. 51 (2002) 35.
[36] M. Sugimoto, H. Katsuno, K. Takatsu, N. Kawata, Zeolites 7 (1987) 503.
[37] H. Liu, L. Su, H. Wang, W. Shen, X. Bao, Y. Xu, Appl. Catal. A 236 (2002) 263.
[38] M. Kentgens, J. Scholl, S. Veeman, J. Phys. Chem. 87 (1983) 4357.
[39] N.Y. Topsoe, K. Pedersen, E.G. Derouane, J. Catal. 70 (1981) 41.
[40] C.V. Hidalgo, H. Itoh, T. Hattori, M. Niwa, Y. Murakami, J. Catal. 85 (1984) 362.
[41] N.R. Meshram, S.G. Hegde, S.B. Kulkarni, Zeolites 6 (1986) 434.
[42] L.J. Lobree, I.Ch. Hwang, J.A. Reimer, A.T. Bell, J. Catal. 186 (1999) 242.
[43] K.H. Schnabel, C. Peuker, B. Parlitz, E. Loffler, U. Kurschner, H.Z. Kriegsmann, J. Phys. Chem. 268 (1987) 225.
[44] K. Chao, B. Chiou, C. Cho, S. Jeng, Zeolites 4 (1984) 2.
[45] D. Freude, J. Klinowski, Chem. Commun. (1988) 1411.
[46] J. Klinowski, Chem. Rev. 91 (1991) 1459.
[47] L.W. Beck, J.L. White, J.F. Haw, J. Am. Chem. Soc. 116 (1994) 9657.
[48] M. Hunger, Catal. Rev. Sci. Eng. 39 (1997) 345.
[49] E. Brunner, H. Ernst, D. Freude, T. Frohlich, M. Hunger, H. Pfeiffer, J. Catal. 127 (1991) 34.
[50] M. Muller, G.HarveyR. Pins, Micropor. Mesopor. Mater. 34 (2000) 135.
[51] M. Hunger, D. Freude, H. Pfeifei, J. Chem. Soc. Faraday Trans. 87 (1991) 657.